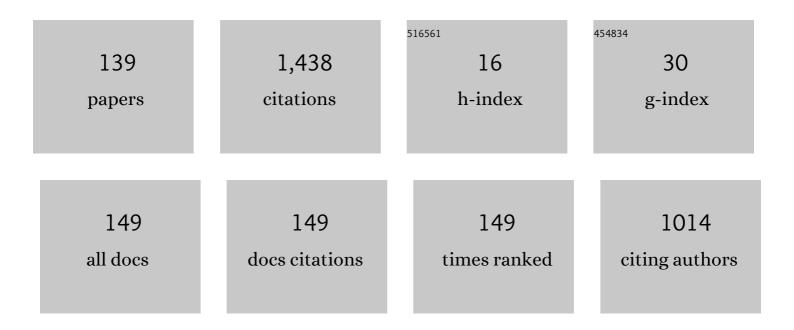
Paul Leroux

List of Publications by Year in descending order

Source: https://exaly.com/author-pdf/3252614/publications.pdf Version: 2024-02-01



#	Article	IF	CITATIONS
1	Radiation-Tolerant Digitally Controlled Ring Oscillator in 65-nm CMOS. IEEE Transactions on Nuclear Science, 2022, 69, 17-25.	1.2	8
2	Characterization of the Total Charge and Time Duration for Single-Event Transient Voltage Pulses in a 65-nm CMOS Technology. IEEE Transactions on Nuclear Science, 2022, 69, 1593-1601.	1.2	4
3	Improvements of portable energy dispersive Xâ€ray fluorescence instrument: Resolution with <scp>Silicon Drift Detector</scp> , measurements stability using pyroelectric sources, and adaptation for space use. X-Ray Spectrometry, 2022, 51, 388-393.	0.9	3
4	A radiation tolerant clock generator for the CMS endcap timing layer readout chip. Journal of Instrumentation, 2022, 17, C03038.	0.5	2
5	TID Sensitivity Assessment of Quadrature LC-Tank VCOs Implemented in 65-nm CMOS Technology. Electronics (Switzerland), 2022, 11, 1399.	1.8	1
6	Impact of Aging Degradation on Heavy-Ion SEU Response of 28-nm UTBB FD-SOI Technology. IEEE Transactions on Nuclear Science, 2022, 69, 1865-1875.	1.2	2
7	Pseudo-Differential Time-Domain Integrator Using Charge-Based Time-Domain Circuits. , 2021, , .		5
8	Single-Event Latchup sensitivity: Temperature effects and the role of the collected charge. Microelectronics Reliability, 2021, 119, 114087.	0.9	2
9	Low-power electronic technologies for harsh radiation environments. Nature Electronics, 2021, 4, 243-253.	13.1	39
10	Study of SEU Sensitivity of SRAM-Based Radiation Monitors in 65-nm CMOS. IEEE Transactions on Nuclear Science, 2021, 68, 913-920.	1.2	14
11	Assessment of Proton Direct Ionization for the Radiation Hardness Assurance of Deep Submicron SRAMs Used in Space Applications. IEEE Transactions on Nuclear Science, 2021, 68, 937-948.	1.2	20
12	A 0.18 pJ/Step Time-Domain 1st Order ΔΣ Capacitance-to-Digital Converter in 65-nm CMOS. , 2021, , .		0
13	A High-Reliability Redundancy Scheme for Design of Radiation-Tolerant Half-Duty Limited DC-DC Converters. Electronics (Switzerland), 2021, 10, 1146.	1.8	2
14	A Review of Semiconductor Based Ionising Radiation Sensors Used in Harsh Radiation Environments and Their Applications. Radiation, 2021, 1, 194-217.	0.6	24
15	Tradeoffs in Time-to-Digital Converter Architectures for Harsh Radiation Environments. IEEE Transactions on Instrumentation and Measurement, 2021, 70, 1-10.	2.4	5
16	Single-Event Effect Responses of Integrated Planar Inductors in 65-nm CMOS. IEEE Transactions on Nuclear Science, 2021, 68, 2587-2597.	1.2	7
17	Radiation-Tolerant All-Digital PLL/CDR with Varactorless LC DCO in 65 nm CMOS. Electronics (Switzerland), 2021, 10, 2741.	1.8	5
18	A Low Noise Fault Tolerant Radiation Hardened 2.56 Gbps Clock-Data Recovery Circuit With High Speed Feed Forward Correction in 65 nm CMOS. IEEE Transactions on Circuits and Systems I: Regular Papers, 2020, 67, 1438-1446.	3.5	11

#	Article	IF	CITATIONS
19	Characterization of a gigabit transceiver for the ATLAS inner tracker pixel detector readout upgrade. Journal of Instrumentation, 2020, 15, T03005-T03005.	0.5	5
20	Methods for clock signal characterization using FPGA resources. Journal of Instrumentation, 2020, 15, P03012-P03012.	0.5	1
21	Reliability-driven pin assignment optimization to improve in-orbit soft-error rate. Microelectronics Reliability, 2020, 114, 113885.	0.9	Ο
22	1.28 and 5.12 Gbps multi-channel twinax cable receiver ASICs for the ATLAS Inner Tracker Pixel Detector upgrade. Nuclear Instruments and Methods in Physics Research, Section A: Accelerators, Spectrometers, Detectors and Associated Equipment, 2020, 981, 164439.	0.7	3
23	Design exploration of majority voter architectures based on the signal probability for TMR strategy optimization in space applications. Microelectronics Reliability, 2020, 114, 113877.	0.9	5
24	Effect of Temperature on Single Event Latchup Sensitivity. , 2020, , .		4
25	Exploiting Transistor Folding Layout as RHBD Technique Against Single-Event Transients. IEEE Transactions on Nuclear Science, 2020, 67, 1581-1589.	1.2	4
26	Mitigation and Predictive Assessment of SET Immunity of Digital Logic Circuits for Space Missions. Aerospace, 2020, 7, 12.	1.1	5
27	The lpGBT PLL and CDR Architecture, Performance and SEE Robustness. , 2020, , .		12
28	Design of a 4 ps radiation hardened TDC with an improved interpolation technique. , 2020, , .		1
29	Practical Driving Electronics for an AOTF-Based NO2 Camera. IEEE Transactions on Instrumentation and Measurement, 2019, 68, 874-881.	2.4	0
30	Impact of Complex Logic Cell Layout on the Single-Event Transient Sensitivity. IEEE Transactions on Nuclear Science, 2019, 66, 1465-1472.	1.2	7
31	Radiation Tolerant Electronics. Electronics (Switzerland), 2019, 8, 730.	1.8	5
32	Radiation hardening efficiency of gate sizing and transistor stacking based on standard cells. Microelectronics Reliability, 2019, 100-101, 113457.	0.9	8
33	A gigabit transceiver for the ATLAS inner tracker pixel detector readout upgrade. Journal of Instrumentation, 2019, 14, C07005-C07005.	0.5	3
34	A bipolar shaping amplifier for high capacitance silicon detectors. Journal of Instrumentation, 2019, 14, P08016-P08016.	0.5	1
35	Radiation Assessment of a 15.6ps Single-Shot Time-to-Digital Converter in Terms of TID. Electronics (Switzerland), 2019, 8, 558.	1.8	7
36	A Novel Modular Radiation Hardening Approach Applied to a Synchronous Buck Converter. Electronics (Switzerland), 2019, 8, 513.	1.8	25

#	Article	IF	CITATIONS
37	A Low Noise Fault Tolerant Radiation Hardened 2.56 Gbps Clock-Data Recovery Circuit with High Speed Feed Forward Correction in 65 nm CMOS. , 2019, , .		5
38	An SRAM-Based Radiation Monitor With Dynamic Voltage Control in 0.18- <inline-formula> <tex-math notation="LaTeX">\$mu\$ </tex-math> </inline-formula> m CMOS Technology. IEEE Transactions on Nuclear Science, 2019, 66, 282-289.	1.2	14
39	A Delay Locked Loop for Time-to-Digital Converters with Quick Recovery and Low Hysteresis. , 2019, , .		1
40	A bipolar shaping amplifier for low background alpha/beta counters with silicon detectors , 2019, , .		0
41	Radiation Hardened CMOS Integrated Circuits for Time-Based Signal Processing. Analog Circuits and Signal Processing Series, 2018, , .	0.3	2
42	A 2.56-GHz SEU Radiation Hard \$LC\$ -Tank VCO for High-Speed Communication Links in 65-nm CMOS Technology. IEEE Transactions on Nuclear Science, 2018, 65, 407-412.	1.2	34
43	Radiation Effects in CMOS Technology. Analog Circuits and Signal Processing Series, 2018, , 1-20.	0.3	5
44	VFAT3: A Trigger and Tracking Front-end ASIC for the Binary Readout of Gaseous and Silicon Sensors. , 2018, , .		4
45	Analysis of the charge sharing effect in the SET sensitivity of bulk 45â€ ⁻ nm standard cell layouts under heavy ions. Microelectronics Reliability, 2018, 88-90, 920-924.	0.9	12
46	Radiation Tolerant, Low Noise Phase Locked Loops in 65 nm CMOS Technology. EPJ Web of Conferences, 2018, 170, 01021.	0.1	1
47	Operational Experience With the GEM Detector Assembly Lines for the CMS Forward Muon Upgrade. IEEE Transactions on Nuclear Science, 2018, 65, 2808-2816.	1.2	3
48	Time-Domain Signal Processing. Analog Circuits and Signal Processing Series, 2018, , 21-42.	0.3	0
49	Low Jitter Clock Generators. Analog Circuits and Signal Processing Series, 2018, , 97-121.	0.3	0
50	Clock Synthesizers. Analog Circuits and Signal Processing Series, 2018, , 43-70.	0.3	0
51	Single Shot Time-to-Digital Converters. Analog Circuits and Signal Processing Series, 2018, , 71-96.	0.3	0
52	Radiation Experiments on CMOS PLLs. Analog Circuits and Signal Processing Series, 2018, , 123-143.	0.3	0
53	Radiation Hard Frequency Synthesizers. Analog Circuits and Signal Processing Series, 2018, , 145-154.	0.3	0
54	A 2.56 GHz Radiation Hard Phase Locked Loop ASIC for High Speed Serial Communication Links. , 2018, , .		0

3

#	Article	IF	CITATIONS
55	Highly broadband circular polarized patch antenna with 3 phase feed structure. , 2017, , .		3
56	Monostatic continuous-wave radar integrating a tunable wideband leakage canceler for indoor tagless localization. International Journal of Microwave and Wireless Technologies, 2017, 9, 1583-1590.	1.5	7
57	High-speed single cable synchronization system for data-converters. Analog Integrated Circuits and Signal Processing, 2017, 90, 283-290.	0.9	Ο
58	Comparison of a 65 nm CMOS Ring- and LC-Oscillator Based PLL in Terms of TID and SEU Sensitivity. IEEE Transactions on Nuclear Science, 2017, 64, 245-252.	1.2	46
59	Highly Tunable Triangular Wave UWB Baseband Pulse Generator With Amplitude Stabilization in 40-nm CMOS. IEEE Transactions on Circuits and Systems II: Express Briefs, 2017, 64, 505-509.	2.2	4
60	Testing of a possible RF-generator for a space based AOTF application in the frame of an ESA space mission. , 2017, , .		1
61	Low-noise and low-power front-end in 130 nm CMOS for triple-GEM detectors supporting wide range of detector capacitances with gain and peaking time programmability , 2017, , .		Ο
62	A Verification Platform to provide the Functional, Characterization and Production testing for the VFAT3 ASIC. , 2017, , .		0
63	A single-event upset robust, 2.2 GHz to 3.2 GHz, 345 fs jitter PLL with triple-modular redundant phase detector in 65 nm CMOS. , 2016, , .		18
64	A low noise clock generator for high-resolution time-to-digital convertors. Journal of Instrumentation, 2016, 11, C02038-C02038.	0.5	4
65	Biomedical wireless radar sensor network for indoor emergency situations detection and vital signs monitoring. , 2016, , .		8
66	Radar range improvement using gradient-free optimization for health care applications. , 2016, , .		3
67	A Self-Calibrated Bang–Bang Phase Detector for Low-Offset Time Signal Processing. IEEE Transactions on Circuits and Systems II: Express Briefs, 2016, 63, 453-457.	2.2	10
68	A MGy, Low-Offset Programmable Instrumentation Amplifier IC for Nuclear Applications. , 2015, , .		3
69	MGy Radiation Assessment of a Space-Graded Amplifier and ADC. , 2015, , .		2
70	The VFAT3-Comm-Port: a complete communication port for front-end ASICs intended for use within the high luminosity radiation environments of the LHC. Journal of Instrumentation, 2015, 10, C03019-C03019.	0.5	3
71	Experimental validation of a compact model for EM reflection and transmission in multi-layered structures. , 2015, , .		0

A 280 ps - 7.5 ns UWB Pulse Generator with Amplitude Compensation in 40 nm CMOS. , 2015, , .

#	Article	IF	CITATIONS
73	A 1 MGy TID Radiation-Tolerant 56 µW CMOS Temperature Sensor with ±1.7°C Accuracy. , 2015, , .		0
74	Embedded DSP-Based Telehealth Radar System for Remote In-Door Fall Detection. IEEE Journal of Biomedical and Health Informatics, 2015, 19, 92-101.	3.9	78
75	Direct RF Subsampling Receivers Enabling Impulse-Based UWB Signals for Breast Cancer Detection. IEEE Transactions on Circuits and Systems II: Express Briefs, 2015, 62, 144-148.	2.2	4
76	RF-driving of acoustic-optical tunable filters; design, realization and qualification of analog and digital modules for ESA. Microelectronics Reliability, 2015, 55, 2103-2107.	0.9	3
77	Highly adjustable mixerâ€based UWB pulse generator architecture with leakage compensation integrated in 40Ânm CMOS. Electronics Letters, 2015, 51, 183-185.	0.5	4
78	A single shot TDC with 4.8 ps resolution in 40 nm CMOS for high energy physics applications. Journal of Instrumentation, 2015, 10, C01031-C01031.	0.5	9
79	Qualification method for a 1 MGy-tolerant front-end chip designed in 65 nm CMOS for the read-out of remotely operated sensors and actuators during maintenance in ITER. Fusion Engineering and Design, 2015, 96-97, 1002-1005.	1.0	9
80	Real-time fall detection and tagless localization using radar techniques. , 2015, , .		5
81	Dual-mode wireless sensor network for real-time contactless in-door health monitoring. , 2015, , .		7
82	Background on Time-to-Digital Converters. Analog Circuits and Signal Processing Series, 2015, , 15-23.	0.3	2
83	A 6-b UWB subsampling track & hold with 5.5-GHz ERBW in 40 nm CMOS. , 2014, , .		3
84	Design of a MGy radiation tolerant resolver-to-digital convertor IC for remotely operated maintenance in harsh environments. Fusion Engineering and Design, 2014, 89, 2314-2319.	1.0	12
85	Analysis of an Indoor Biomedical Radar-Based System for Health Monitoring. IEEE Transactions on Microwave Theory and Techniques, 2013, 61, 2061-2068.	2.9	147
86	A practical distance measurement improvement technique for a SFCW-based health monitoring radar. , 2013, , .		3
87	A 63,000 Q-factor relaxation oscillator with switched-capacitor integrated error feedback. , 2013, , .		42
88	Optimized SFCW radar sensor aiming at fall detection in a real room environment. , 2013, , .		18
89	A 4.5 MGy TID-Tolerant CMOS Bandgap Reference Circuit Using a Dynamic Base Leakage Compensation Technique. IEEE Transactions on Nuclear Science, 2013, 60, 2819-2824.	1.2	22
90	17 bit 4.35mW 1kHz Delta Sigma ADC and 256-to-1 multiplexer for remote handling instrumentation equipment. Fusion Engineering and Design, 2013, 88, 1942-1946.	1.0	9

Paul Leroux

#	Article	IF	CITATIONS
91	FPGA based flexible UWB pulse transmitter using EM subtraction. Electronics Letters, 2013, 49, 1243-1244.	0.5	5
92	A > 4 MGy radiation tolerant 8 THzOhm transimpedance amplifier with 50 dB dynamic range. Journal of Instrumentation, 2013, 8, C02052-C02052.	0.5	1
93	Design and implementation of an ultrasonic local positioning system for robot guidance in a heavy liquid metal environment. , 2013, , .		1
94	Design and functional validation of a complex impedance measurement device for characterization of ultrasonic transducers. , 2013, , .		3
95	Conceptual design of a MGy tolerant integrated signal conditioning circuit in 130nm and 700nm CMOS. Journal of Instrumentation, 2012, 7, C01017-C01017.	0.5	4
96	Optimised waveform design for radar sensor aimed at contactless health monitoring. Electronics Letters, 2012, 48, 1255.	0.5	14
97	Design and Simulation of a MGy Radiation Tolerant Signal Conditioning Circuit for Resistive Sensors in 0.7 \$mu\$m CMOS. IEEE Transactions on Nuclear Science, 2012, 59, 1309-1316.	1.2	2
98	SFCW microwave radar for in-door fall detection. , 2012, , .		39
99	Design and Assessment of a 6 ps-Resolution Time-to-Digital Converter With 5 MGy Gamma-Dose Tolerance for LIDAR Application. IEEE Transactions on Nuclear Science, 2012, 59, 1382-1389.	1.2	23
100	1-1-1 MASH \$Delta Sigma\$ Time-to-Digital Converters With 6 ps Resolution and Third-Order Noise-Shaping. IEEE Journal of Solid-State Circuits, 2012, 47, 2093-2106.	3.5	50
101	Conceptual design of a versatile radiation tolerant integrated signal conditioning circuit for resistive sensors. , 2011, , .		0
102	Design of a MGy tolerant instrumentation amplifier using a correlated double sampling technique in 130 nm CMOS. , 2011, , .		2
103	Design and assessment of a 6 ps-resolution time-to-digital converter with 5 MGy gamma-dose tolerance for nuclear instrumentation. , 2011, , .		1
104	A 0.7mW 13b temperature-stable MASH ΔΣ TDC with delay-line assisted calibration. , 2011, ,		7
105	A 1.7mW 11b 1–1–1 MASH ΔΣ time-to-digital converter. , 2011, , .		15
106	Ultra-wideband antipodal vivaldi antenna array with Wilkinson power divider feeding network. , 2011, ,		4
107	Radiation effects upon the mismatch of identically laid out transistor pairs. , 2011, , .		8
108	Design and assessment of a robust voltage amplifier with 2.5 GHz GBW and >100 kGy total dose tolerance. Journal of Instrumentation, 2011, 6, C01076-C01076.	0.5	3

#	Article	IF	CITATIONS
109	0.7μm CMOS digitally controlled switched capacitor oscillator for a resonance tracking ultrasound transmitter. , 2011, , .		0
110	Influence of Back-Gate Bias and Process Conditions on the Gamma Degradation of the Transconductance of MuGFETs. IEEE Transactions on Nuclear Science, 2010, 57, 1771-1776.	1.2	16
111	Effect of rotation, gate-dielectric and SEG on the noise behavior of advanced SOI MuGFETs. Solid-State Electronics, 2010, 54, 178-184.	0.8	12
112	Measuring material/tissue permittivity by UWB Time-domain Reflectometry techniques. , 2010, , .		4
113	Influence of Fin Width on the Total Dose Behavior of p-Channel Bulk MuGFETs. IEEE Electron Device Letters, 2010, 31, 243-245.	2.2	26
114	Effect of Airgap Deep Trench Isolation on the Gamma Radiation Behavior of a 0.13 \$mu{hbox {m}}\$ SiGe:C NPN HBT Technology. IEEE Transactions on Nuclear Science, 2009, 56, 2198-2204.	1.2	6
115	Modeling, Design, Assessment of a 0.4 \$mu{hbox {m}}\$ SiGe Bipolar VCSEL Driver IC Under \$gamma \$-Radiation. IEEE Transactions on Nuclear Science, 2009, 56, 1920-1925.	1.2	3
116	Influence of back-gate bias and process conditions on the gamma-degradation of the transconductance of MuGFETs. , 2009, , .		0
117	Modelling of γ-radiation effects in bipolar transistors with VHDL-AMS. , 2009, , .		1
118	Design, assessment and modeling of an integrated 0.4 µm SiGe Bipolar VCSEL driver under γ-radiation. , 2008, , .		2
119	Proton and gamma radiation of 0.13 µm 200 GHz NPN SiGe:C HBTs featuring an airgap deep trench isolation. , 2007, , .		3
120	Design and Assessment of a Circuit and Layout Level Radiation Hardened CMOS VCSEL Driver. IEEE Transactions on Nuclear Science, 2007, 54, 1055-1060.	1.2	13
121	Geometry and Strain Dependence of the Proton Radiation Behavior of MuGFET Devices. IEEE Transactions on Nuclear Science, 2007, 54, 2227-2232.	1.2	29
122	SPICE Modelling of a Discrete COTS SiGe HBT for Digital Applications up to MGy Dose Levels. IEEE Transactions on Nuclear Science, 2006, 53, 1945-1949.	1.2	7
123	Design and Assessment of a High Gamma-Dose Tolerant VCSEL Driver With Discrete SiGe HBTs. IEEE Transactions on Nuclear Science, 2006, 53, 2033-2039.	1.2	9
124	ESD–RF co-design methodology for the state of the art RF-CMOS blocks. Microelectronics Reliability, 2005, 45, 255-268.	0.9	11
125	SPICE modelling of a discrete COTS SiGe HBT for digital applications up to MGy dose levels. , 2005, , .		2
126	Design and Assessment of a High Gamma-Dose Tolerant VCSEL Driver wit Discrete SiGe HBT's. European Conference on Radiation and Its Effects on Components and Systems, Proceedings of the, 2005, , .	0.0	2

Paul Leroux

#	Article	IF	CITATIONS
127	High total dose gamma radiation assessment of commercially available SiGe heterojunction bipolar transistors. , 2005, , .		6
128	High ESD performance, low power CMOS LNA for GPS applications. Journal of Electrostatics, 2003, 59, 179-192.	1.0	7
129	RF-ESD Co-Design for High Performance CMOS LNAs. , 2003, , 207-226.		3
130	Optimization of a fully integrated low power CMOS GPS receiver. IEEE/ACM International Conference on Computer-Aided Design, Digest of Technical Papers, 2002, , .	0.0	1
131	A 0.8-dB NF ESD-Protected 9-mW CMOS LNA operating at 1.23 GHz [for GPS receiver]. IEEE Journal of Solid-State Circuits, 2002, 37, 760-765.	3.5	71
132	Low-voltage low-power CMOS-RF transceiver design. IEEE Transactions on Microwave Theory and Techniques, 2002, 50, 281-287.	2.9	72
133	High-performance 5.2 GHz LNA with on-chip inductor to provide ESD protection. Electronics Letters, 2001, 37, 467.	0.5	67
134	A fully-integrated GPS receiver front-end with 40 mW power consumption. , 0, , .		23
135	Optimization of a fully integrated low power CMOS GPS receiver. , 0, , .		1
136	Gigabit photodiodes in standard digital nanometer CMOS technologies. , 0, , .		2
137	Two high-speed optical front-ends with integrated photodiodes in standard 0.18 μm CMOS. , 0, , .		7
138	A 5 GHz CMOS low-noise amplifier with inductive ESD protection exceeding 3 kV HBM. , 0, , .		17
139	RF-ESD design and measurement of CMOS LNAs: a comparison between diode and inductive protection. , 0, , .		1